

RESEARCH

Open Access



Identification of ruptured intracranial aneurysms using the aneurysm-specific prediction score in patients with multiple aneurysms with subarachnoid hemorrhages—a Chinese population based external validation study

Xue-hua Zhang¹, Xiao-yan Zhao¹, Lan-lan Liu², Li Wen² and Guang-xian Wang^{1*}

Abstract

Background: For patients with aneurysmal subarachnoid hemorrhages (SAHs) and multiple intracranial aneurysms (MIAs), a simple and fast imaging method that can identify ruptured intracranial aneurysms (RIAs) may have great clinical value. We sought to use the aneurysm-specific prediction score to identify RIAs in patients with MIAs and evaluate the aneurysm-specific prediction score.

Methods: Between May 2018 and May 2021, 134 patients with 290 MIAs were retrospectively analyzed. All patients had an SAH due to IA rupture. CT angiography (CTA) was used to assess the maximum diameter, shape, and location of IAs to calculate the aneurysm-specific prediction score. Then, the aneurysm-specific prediction score was applied to RIAs in patients with MIAs.

Results: The IAs with the highest aneurysm-specific prediction scores had not ruptured in 17 (12.7%) of the 134 patients with 290 MIAs. The sensitivity, specificity, false omission rate, diagnostic error rate, and diagnostic accuracy of the aneurysm-specific prediction score were higher than those of the maximum diameter, shape, and location of IAs.

Conclusions: The present study suggests that the aneurysm-specific prediction score has high diagnostic accuracy in identifying RIAs in patients with MIAs and SAH, but that it needs further evaluation.

Keywords: Multiple intracranial aneurysms, Subarachnoid hemorrhage, Risk factors, Computed tomography arteriography, Predictive scoring model

Background

Subarachnoid hemorrhage (SAH) caused by a ruptured intracranial aneurysm (RIA) has high mortality and disability rates [1]. RIAs should be treated as soon as possible to prevent rebleeding, and the choice of treatment method (microsurgical clipping or endovascular coiling) depends on the site of the RIA [2]. Approximately 30% of patients with intracranial aneurysms (IAs) have multiple

*Correspondence: wgxlove1234@163.com

¹ Department of Radiology, Banan People's Hospital, Chongqing Medical University, Chongqing 400037, China

Full list of author information is available at the end of the article



IAs (MIAs) [3], and approximately one-third of MIAs have uncertain rupture sources [1]. Misdiagnosis of the location of the RIA may lead to postoperative rebleeding and a poorer outcome [4, 5]. Therefore, it is of great clinical value to accurately determine the RIA in MIAs if all IAs cannot be treated at the same time.

The hemorrhage pattern is generally the primary indicator of RIA; however, it is quite difficult to judge RIAs by diffuse or symmetrical bleeding [6]. Although high-resolution contrast-enhanced magnetic resonance vessel wall imaging helps to identify the site of RIA in patients with MIAs, scan time and spontaneous motion are notable limitations [7]. Some scholars used the population, hypertension, age, size, earlier subarachnoid hemorrhage, aneurysm site (PHASES) score and unruptured intracranial aneurysm treatment score (UIATS) to predict RIA [8–11]. However, all these studies showed that the PHASES score and UIATS had a lower ability to identify RIA.

Recently, Hadjiathanasiou et al. [6] developed a novel prediction score, the aneurysm-specific prediction score, for simple and quick identification of RIAs. Encouragingly, the prediction score correctly identified the RIA

in all the patients. However, it is not clear whether this score is highly applicable to the Chinese population. After all, in terms of genetics, the Chinese and Caucasian are not identical. Hence, we sought to identify whether the aneurysm-specific prediction score is able to predict RIA in the Chinese population.

Methods

Patient population

This retrospective study was approved by the local ethics committee (Banan People’s hospital, 2,021,015; Xinqiao hospital, 2,016,031), which waived the requirement for informed consent from patients. Between May 2018 and May 2021, at two participating centers, consecutive patients with aneurysmal SAH and more than one IA on CTA were included. SAH was diagnosed by non-enhanced CT or lumbar puncture. RIAs were confirmed in two ways: microsurgical clipping or endovascular coiling. In endovascular coiling, RIAs were identified according to hemorrhage pattern or further CT follow-up. The exclusion criteria were as follows: (1) single IA; (2) multiple unruptured IAs but without evident SAH; (3) poor

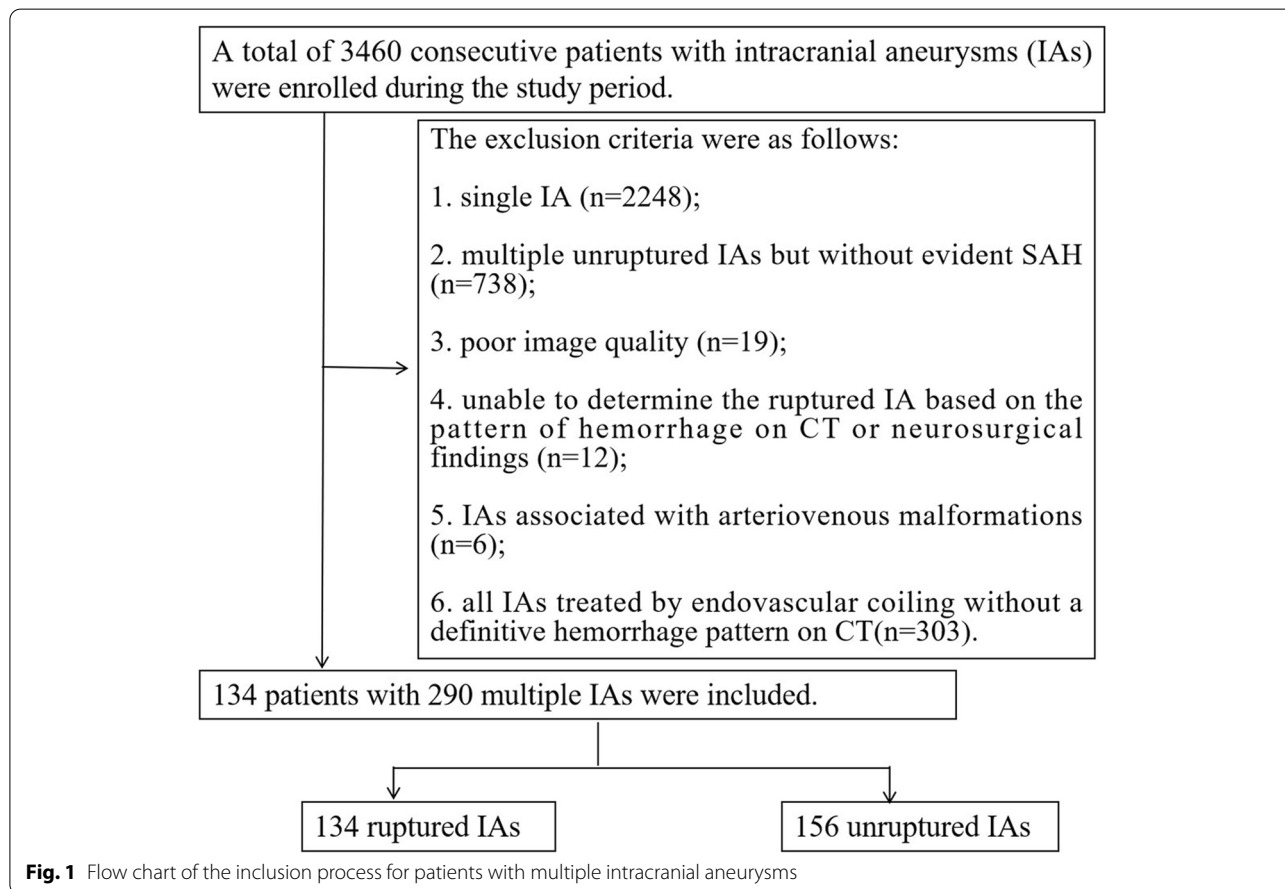


Fig. 1 Flow chart of the inclusion process for patients with multiple intracranial aneurysms

Table 1 Morphological characteristics of the aneurysms

| Morphological characteristics | Unruptured group (n = 156) | Ruptured group (n = 134) | P |
|------------------------------------|----------------------------|--------------------------|---------|
| Maximum diameter (mm) | 5.02 ± 2.44 | 7.88 ± 3.02 | < 0.001 |
| Shape | | | < 0.001 |
| Irregular | 36 (23.1%) | 95 (70.9%) | |
| Regular | 120 (76.9%) | 39 (29.1%) | |
| Location | | | |
| PC | 10 (6.4%) | 5 (3.7%) | 0.427 |
| AcomA + AA | 16 (10.3%) | 24 (17.9%) | 0.063 |
| PcomA | 38 (24.4%) | 63 (47.1%) | < 0.001 |
| MCA | 52 (33.3%) | 33 (24.6%) | 0.121 |
| ICA | 40 (25.6%) | 9 (6.7%) | < 0.001 |
| Aneurysm-specific prediction score | 0.03631 ± 0.40 | 0.56653 ± 0.40 | < 0.001 |

PC Posterior circulation, AcomA Anterior communicating artery, AA Anterior cerebral artery, ICA Internal carotid artery, MCA Middle cerebral artery, PcomA Posterior communicating artery

image quality making it impossible to evaluate the geometric morphology of IAs; (4) inability to determine the RIA based on the pattern of hemorrhage on CT or neurosurgical findings; (5) IAs with vascular malformations; and (6) all IAs were treated by endovascular coiling without a definitive hemorrhage pattern on CT. The patient inclusion flow chart is shown in Fig. 1.

Imaging protocol and analysis

All patients underwent pretreatment nonenhanced CT and CTA on a 320 multidetector (Toshiba Aquilion One; Toshiba Medical Systems, Tokyo, Japan) or 64

multidetector (GE LightSpeed VCT; GE Healthcare, Milwaukee, Wisconsin, USA) machine. The CTA data were reconstructed with a thickness of 0.5 mm or 0.625 mm and postprocessed to generate three-dimensional volume-rendered images.

All images were analyzed by two experienced radiologists (one with 5 years of experience in neuroradiology and the other with 15 years of experience in vascular imaging), who measured the maximum diameter of IAs and determined their shape and location independently. IA shapes were classified as regular or irregular, with lobular aneurysms or aneurysms with a bleb classified

Table 2 Diagnostic accuracy of the morphological characteristics of the IAs and the aneurysm-specific prediction score

| Morphological characteristics | Results | | Total | SEN% | SPE% | β% | α% | DA% |
|------------------------------------|---------|-----|-------|------|------|------|------|------|
| | UIA | RIA | | | | | | |
| Maximum diameter (mm) | | | | | | | | |
| Yes | 25 | 109 | 134 | 81.3 | 83.9 | 18.7 | 16.1 | 82.8 |
| No | 131 | 25 | 156 | | | | | |
| Shape | | | | | | | | |
| Irregular | 36 | 95 | 131 | 70.9 | 76.9 | 29.1 | 23.1 | 74.1 |
| Regular | 120 | 39 | 159 | | | | | |
| Location | | | | | | | | |
| PC | 10 | 5 | 15 | 3.7 | 93.6 | 96.3 | 6.4 | 51.4 |
| AcomA + AA | 16 | 24 | 40 | 17.9 | 89.7 | 82.1 | 10.3 | 56.6 |
| PcomA | 38 | 63 | 101 | 47.0 | 75.6 | 53.0 | 24.4 | 62.4 |
| MCA | 52 | 33 | 85 | 24.6 | 66.7 | 75.4 | 33.3 | 47.2 |
| ICA | 40 | 9 | 49 | 6.7 | 74.4 | 93.3 | 25.6 | 43.1 |
| Aneurysm-specific prediction score | | | | | | | | |
| Largest | 17 | 117 | 134 | 87.3 | 89.1 | 12.7 | 10.9 | 88.3 |
| Nonlargest | 139 | 17 | 156 | | | | | |
| Total | 156 | 134 | 290 | | | | | |

IA Intracranial aneurysm, SEN Sensitivity, SPE Specificity, β False omission rate, α Diagnostic error rate, DA Diagnostic accuracy, UIA Unruptured intracranial aneurysm, RIA Ruptured intracranial aneurysm, PC Posterior circulation, AcomA Anterior communicating artery, AA Anterior cerebral artery, ICA Internal carotid artery, MCA Middle cerebral artery, PcomA Posterior communicating artery

as irregular [6]. IA location is divided into five regions: anterior cerebral artery (AA), including anterior communicating artery (AcomA), internal carotid artery (ICA) excluding posterior communicating artery (PcomA), PcomA, middle cerebral artery (MCA) and posterior circulation (PC) [6]. Maximum diameter was defined as the largest measurement in terms of maximum dome diameter or width [11]. For categorical data, controversial cases were resolved through discussion, and the average values of the continuous data obtained by the two readers were used for analysis.

The maximum diameter, shape and location of IAs were used to calculate the aneurysm-specific prediction score, which is equal to $A + B + C$: $A = 0.0427 \times$ maximum diameter (mm); $B = 0$ if the IA was located at AcomA and AA, -0.0104 if located at PcomA, -0.1831 if located at posterior circulation, -0.4055 if located at MCA, -0.5973 if located at ICA; $C = 0$ if the shape is defined as regular, or 0.5387 if shape is defined as irregular. The aneurysm-specific prediction score was derived from a component-wise gradient boosting algorithm with linear base learners, whose main advantage is the algorithmic procedure of fitting the logistic model (i.e., to estimate its coefficients) [6]. For each patient, the IA with the maximum aneurysm-specific prediction score was predicted as the one that would rupture.

Statistical analysis

SPSS version 17.0 (SPSS Inc., Chicago, IL, USA) was used for all statistical analyses, and a P value less than 0.05 was regarded as statistically significant. The agreement between two observers for the shape and location of the IAs was evaluated by a kappa value. Categorical data and continuous data are expressed as the number of IAs (%) and mean \pm standard deviation, respectively. Categorical data were compared by using the chi-squared test, while continuous data were compared using the independent-samples Student's t test for normally distributed data or the Mann-Whitney U test for nonnormally distributed data. A receiver operating characteristic (ROC) curve was generated to determine the area under the curve.

Results

One hundred and thirty-four patients with 290 MIAs (one ruptured and the other unruptured) were available for analysis (supplementary file). Among the 33 males and 101 females, the mean ages were 59.5 years for all patients, 54.7 years (range, 41–79 years) for males, and 60.9 years (range, 33–86 years) for females. There were 115 patients with 2 IAs, 16 patients with 3 IAs and 3 patients with 4 IAs.

Table 3 The RIAs that were misdiagnosed in 17 patients with 38 MIAs

| Patients | Size (mm) | Location | Shape | Aneurysm-specific prediction score | Ruptured |
|----------|-----------|----------|-----------|------------------------------------|----------|
| 1 | 7.9 | PcomA | Irregular | 0.86563 | No |
| | 7.6 | PcomA | Irregular | 0.85282 | Yes |
| 2 | 5.3 | PcomA | Regular | 0.21591 | No |
| | 3.7 | PcomA | Regular | 0.14759 | Yes |
| 3 | 4.5 | AcomA | Irregular | 0.73085 | No |
| | 4.3 | MCA | Regular | -0.22189 | No |
| 4 | 10.7 | MCA | Irregular | 0.59009 | Yes |
| | 2.4 | PcomA | Irregular | 0.63078 | No |
| 5 | 4.8 | PcomA | Regular | 0.19456 | Yes |
| | 4.7 | PcomA | Irregular | 0.72899 | No |
| 6 | 4.0 | PcomA | Regular | 0.1604 | Yes |
| | 6.9 | MCA | Irregular | 0.42783 | No |
| 7 | 4.1 | MCA | Regular | -0.23043 | Yes |
| | 7.5 | AA | Regular | 0.32025 | No |
| 8 | 6.1 | AcomA | Regular | 0.26047 | Yes |
| | 6.1 | MCA | Irregular | 0.39367 | No |
| 9 | 8.4 | ICA | Regular | -0.23862 | Yes |
| | 7.3 | MCA | Irregular | 0.44491 | No |
| 10 | 3.7 | PcomA | Regular | 0.14759 | Yes |
| | 4.3 | PcomA | Regular | 0.17321 | No |
| 11 | 5.3 | ICA | Regular | -0.37099 | Yes |
| | 7.4 | AcomA | Irregular | 0.85468 | No |
| 12 | 14 | ICA | Irregular | 0.5392 | Yes |
| | 5.1 | AcomA | Regular | 0.21777 | No |
| 13 | 3.6 | MCA | Regular | -0.25178 | Yes |
| | 5.4 | PcomA | Regular | 0.22018 | No |
| 14 | 11.6 | MCA | Regular | 0.08982 | Yes |
| | 3.3 | ICA | Regular | -0.45639 | No |
| 15 | 3 | ICA | Regular | -0.4692 | Yes |
| | 6.8 | MCA | Irregular | 0.42356 | No |
| 16 | 5.4 | PcomA | Irregular | 0.75888 | No |
| | 6.7 | PcomA | Regular | 0.27569 | Yes |
| 17 | 7 | PcomA | Irregular | 0.8272 | No |
| | 5.7 | PcomA | Irregular | 0.77169 | Yes |
| 17 | 2.8 | MCA | Regular | -0.28594 | No |
| | 7.1 | PcomA | Irregular | 0.83147 | No |
| | 3 | ICA | Regular | -0.4692 | No |
| | 6.6 | PcomA | Irregular | 0.81012 | Yes |

RIAs Ruptured intracranial aneurysms, MIA Multiple intracranial aneurysms, AA Anterior cerebral artery, AcomA Anterior communicating artery, ICA Internal carotid artery, PcomA Posterior communicating artery, MCA Middle cerebral artery

Interobserver agreement on the CTA categorical factors was good ($k = 0.951$ for the shape of the IAs, $k = 1.000$ for the location of IAs). Table 1 summarizes the morphological characteristics of the IAs. The

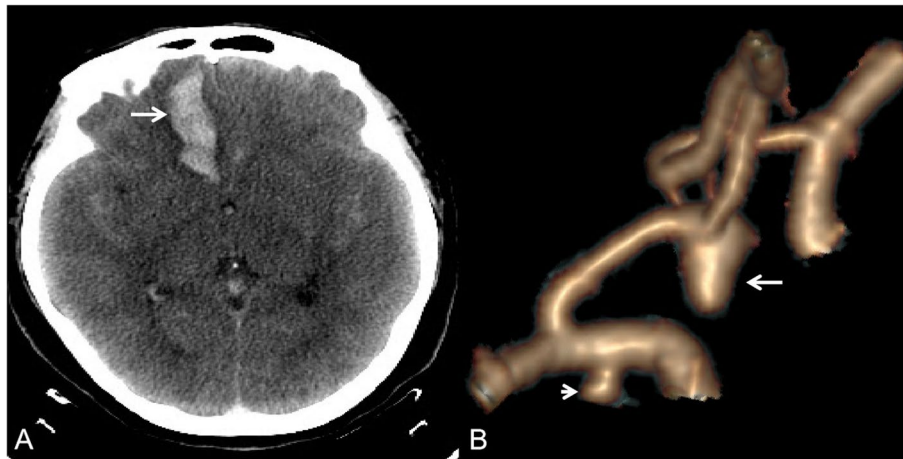


Fig. 2 A 52-year-old female presented with severe headache. CT scan showed subarachnoid hemorrhage with a focal hematoma (arrow). Computed tomography angiography showed a ruptured anterior communicating artery aneurysm (large arrow, aneurysm-specific prediction score = 0.90592) and an unruptured internal carotid artery aneurysm (small arrow, aneurysm-specific prediction score = -0.42223)

mean maximum diameter was 6.34 ± 3.07 mm (range, 1.8–20.7 mm). The mean aneurysm-specific prediction score was 0.28131 ± 0.48 (range, -0.49909–1.24993). The maximum diameter, irregular shape, location in the PcomA and ICA, and aneurysm-specific prediction score were significantly different between the ruptured and unruptured groups.

The diagnostic accuracy of the morphological characteristics of the IAs and the aneurysm-specific prediction score are listed in Table 2. When using maximum diameter alone, the sensitivity, specificity, false omission rate, diagnostic error rate, and diagnostic accuracy were 81.3%, 83.9%, 18.7%, 16.0% and 82.8%, respectively. When using irregular shape alone, the sensitivity, specificity, false omission rate, diagnostic error rate, and diagnostic accuracy were 29.1%, 23.0%, 70.8%,

76.9% and 25.7%, respectively. When using IA location alone, the overall diagnostic accuracy was 43.1–62.4%. When using the aneurysm-specific prediction score, the RIAs were misdiagnosed in 17 patients with 38 MIAs (Table 3). Six RIAs had a large maximum diameter, but due to the location and shape of IAs, the aneurysm-specific prediction score was reduced (Figs. 2 and 3). The sensitivity, specificity, false omission rate, diagnostic error rate, and diagnostic accuracy of the aneurysm-specific prediction score were 87.3%, 89.1%, 12.7%, 10.9%, and 88.3%, respectively.

The ROC analysis was performed for continuous data. The areas under the curve for maximum diameter, location, shape and the aneurysm-specific prediction score were 0.798, 0.536, 0.736 and 0.781, respectively (Fig. 4 and Table 4).

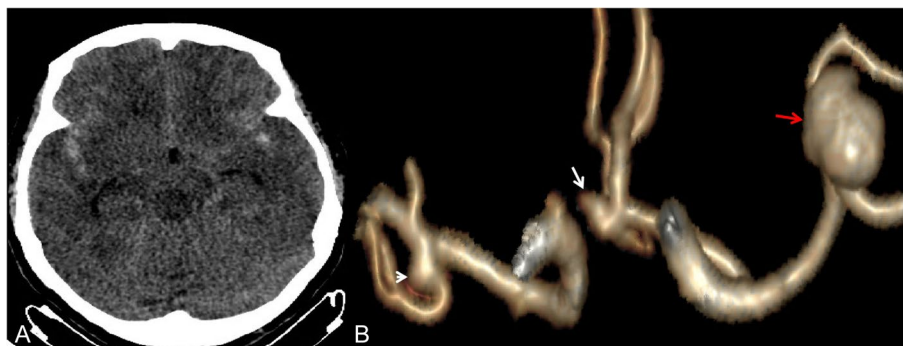
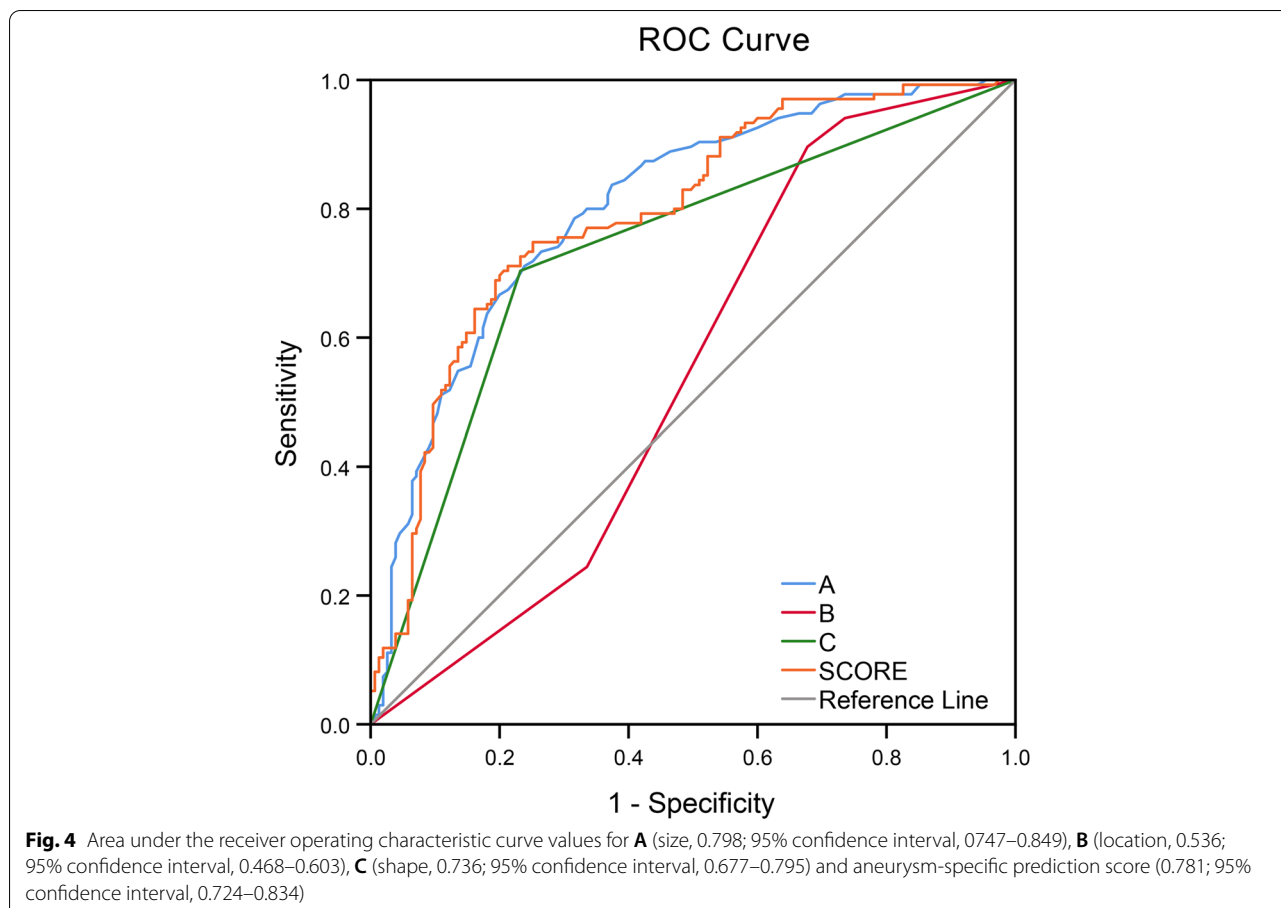


Fig. 3 A 62-year-old female presented with symmetrical subarachnoid hemorrhage. Computed tomography angiography showed three IAs located at the left middle cerebral artery (red arrow, ruptured, aneurysm-specific prediction score = 0.59009), right middle cerebral artery (small arrow, unruptured, aneurysm-specific prediction score = -0.22189), and anterior communicating artery (larger arrow, unruptured, aneurysm-specific prediction score = 0.73085)



Discussion

The aneurysm-specific prediction score was established according to IA size, location and shape and was developed to identify RIAs in SAH patients harboring MIAs [6]. In this study, we applied the aneurysm-specific prediction score in 134 SAH patients with MIAs and found that the sensitivity, specificity, false omission rate, diagnostic error rate, and diagnostic accuracy were 87.3%, 89.1%, 12.7%, 10.9%, and 88.3%, respectively.

Table 4 Area under the curve analysis for A, B, C and the aneurysm-specific prediction score

| Characteristic | Area | P | 95% confidence interval |
|------------------------------------|-------|---------|-------------------------|
| A | 0.798 | < 0.001 | 0.747–0.849 |
| B | 0.536 | 0.297 | 0.468–0.603 |
| C | 0.736 | < 0.001 | 0.677–0.795 |
| Aneurysm-specific prediction score | 0.781 | < 0.001 | 0.728–0.834 |

A, size = 0.0427 × maximum diameter of aneurysm (mm); B, location = 0, -0.0104, -0.1831, -0.4055, or -0.5973; C, shape = 0 or 1

Traditionally, size has been considered an important factor in IA rupture, and a large IA is considered more prone to rupture than a small IA. Some studies have reported that size is a significant predictive factor for IA rupture [12, 13]. Although Björkman et al. [14] indicated that IA size was associated with IA rupture, the RIA was not of the largest size in 13% of their study cohort, and they found that irregular shape may identify the RIA better than size in patients presenting with SAH and MIAs. In addition, Backes et al. [2] reported that RIA was not the largest IA in 29% of patients with MIAs. In this study, 18.7% (25/134) of the patients had an unruptured IA with the largest diameter, and 15 of them did not have the largest aneurysm-specific prediction score.

Irregular shape was thought to be associated with IA rupture [12, 13], possibly because the irregular shape increases the local hemodynamic stress [15]. Backes et al. [2] reported that irregular shape is associated with IA rupture independent of IA size and location and independent of patient characteristics. Björkman et al. [14] showed that shape and size had the best diagnostic value for identifying RIAs in patients

presenting with SAH and MIAs, but shape may be better than size. However, Orning et al. [4] reported that it is unreliable to use morphological features of IA in determining rupture sites in nondefinitive SAH patterns. Another study also showed that morphological and hemodynamic parameters seem to have no or only low effect on the prediction of RIA in patients with MIAs [16]. The present results showed that 39 (29.1%) RIAs had regular shapes, and 36 (23.1%) unruptured IAs had irregular shapes.

IAs located in the AcomA, PcomA, or PC are considered to have a high risk of rupture [17–19]. The American Heart Association/American Stroke Association indicated that the treatment decision regarding UIAs is based mainly on the size and location [20]. In this study, PcomA, AcomA and MCA were the most common sites in aneurysmal SAH patients. These results are consistent with previous study [21]. Although IAs located in the PcomA ruptured more often than IAs in other locations, the diagnostic accuracy was only 62.4%.

The aim in developing the aneurysm-specific prediction scoring system was to identify RIAs in SAH patients with MIAs, and the prediction score had high accuracy in a small prospective sample [6]. In this study, the aneurysm-specific prediction score had high sensitivity and specificity, but 17 UIAs were misdiagnosed as RIAs. On the other hand, the area under the curve of the aneurysm-specific prediction score was lower than that of maximum diameter, indicating that the performance of the aneurysm-specific prediction score was not satisfactory. One of the reasons is that IA size and shape may change after rupture. Another reason is the inherent flaws of the aneurysm-specific prediction scoring system: sometimes the location and shape of IAs may lead to a decrease in the aneurysm-specific prediction score. The coefficients need to be optimized to further improve the rate of recognition of RIAs. In addition, morphological characteristics such as location of bifurcation, small-diameter of the parent artery, and location of the AcomA with A1 dominance are risk factors for IA rupture [22, 23]. Some studies reported that an aspect ratio ≥ 1.3 or the size ratio were the best factor for identifying RIAs [2, 24]. Finally, different populations may lead to different results. It is well known that Japanese and Finnish patients have a higher risk of IA rupture than those from other geographic regions [25]. While, a nationwide epidemiological in China showed that among the patients with aneurysmal SAH, only 15.4% had MIAs [21], which less than Caucasian and Japanese population [17, 26].

Limitations

The present study had a limitations. First, the shape or size of the RIAs might have changed due to the rupture, and the results may be biased. Second, this study considered only MIAs with SAH, and the results may not be applicable to patients with a single IA or unruptured MIAs. Third, as we used CTA data in this study, conus arteriosus could have been misdiagnosed as an IA, causing a patient with a single real IA to be identified as one with “MIAs,” although this situation is unlikely. Fourth, the sample size is relatively small in this study, half of the size of the originally published cohort by Hadjiathanasiou et al. [6]. Last, this study only validated the accuracy of the aneurysm-specific prediction scoring system and did not compare it with other scoring systems. A multicenter prospective study with a large sample size is needed in the future.

Conclusions

We applied the aneurysm-specific prediction score to Chinese patients with MIAs and SAH to identify RIAs and found that the scoring system had high diagnostic accuracy but was not perfect. Larger cohorts for prospective evaluation are warranted in the future.

Supplementary Information

The online version contains supplementary material available at <https://doi.org/10.1186/s12883-022-02727-w>.

Additional file 1.

Acknowledgements

The authors thank American Journal Experts (AJE) for assisting in the preparation of this paper.

Authors' contributions

Guang-xian Wang designed the study. Xue-hua Zhang, Lan-lan Liu and Li Wen collected, analyzed and interpreted data. X-H Zhang wrote the initial paper and G-X Wang revised the paper. Xiao-yan Zhao performed statistical analyses. Xiao-yan Zhao, Lan-lan Liu and Li Wen revised the paper for intellectual content. All authors read and approved the final manuscript.

Funding

This study was supported by the Science and Technology Commission of Chongqing City, China (no.cstc2019jcyj-msxmX0323) and the Joint Project of Science and Health of Chongqing City, China (2021MSXM030).

Availability of data and materials

All data generated or analysed during this study are included in this published article and its supplementary information files.

Declarations

Ethics approval and consent to participate

All aspects of this study were approved by the ethics committee of the Banan People's Hospital, Chongqing Medical University, Chongqing, China (No.:2021015). The requirement for informed consent is waived by the ethics committee of the Banan People's Hospital, Chongqing Medical University, Chongqing, China. All procedures performed in studies involving human participants were in accordance with the ethical standards of the institutional

and national research committee and with the 1964 Helsinki declaration and its later amendments or comparable ethical standards.

Consent for publication

Not applicable.

Competing interests

The authors declare that they have no competing interests.

Author details

¹Department of Radiology, Banan People's Hospital, Chongqing Medical University, Chongqing 400037, China. ²Department of Radiology, Army Medical University Xinqiao Hospital, Chongqing 400037, China.

Received: 3 February 2022 Accepted: 17 May 2022

Published online: 01 June 2022

References

1. Yao A, Jia L, Li J, Wang B, Zhang J, Xue Z, et al. Fusion of subarachnoid hemorrhage data and computed tomography angiography data is helpful to identify the rupture source in patients with multiple intracranial aneurysms. *Neurosurg Focus*. 2021;44:1411–6.
2. Backes D, Vergouwen MD, Velthuis BK, van der Schaaf IC, Bor AS, Algra A, et al. Difference in aneurysm characteristics between ruptured and unruptured aneurysms in patients with multiple intracranial aneurysms. *Stroke*. 2014;45:1299–303.
3. Bhogal P, AlMatter M, Hellstern V, Ganslandt O, Bözner H, Henkes H, et al. Difference in aneurysm characteristics between ruptured and unruptured aneurysms in patients with multiple intracranial aneurysms. *Surg Neurol Int*. 2018;9:1.
4. Orning JL, Shakur SF, Alaraj A, Behbahani M, Charbel FT, Aletich VA, et al. Accuracy in Identifying the Source of Subarachnoid Hemorrhage in the Setting of Multiple Intracranial Aneurysms. *Neurosurgery*. 2018;83:62–8.
5. Karttunen AI, Jartti PH, Ukkola VA, Sajanti J, Haapea M. Value of the quantity and distribution of subarachnoid haemorrhage on CT in the localization of a ruptured cerebral aneurysm. *Acta Neurochir (Wien)*. 2003;145:655–61.
6. Hadjiathanasiou A, Schuss P, Brandecker S, Welchowski T, Schmid M, Vatter H, et al. Multiple aneurysms in subarachnoid hemorrhage-identification of the ruptured aneurysm, when the bleeding pattern is not self-explanatory-development of a novel prediction score. *BMC Neurol*. 2020;20:70.
7. Omodaka S, Endo H, Niizuma K, Fujimura M, Endo T, Sato K, Sugiyama SI, Inoue T, Tominaga T. Circumferential Wall Enhancement on Magnetic Resonance Imaging is Useful to Identify Rupture Site in Patients with Multiple Cerebral Aneurysms. *Neurosurgery*. 2018;82:638–44.
8. Feghali J, Gami A, Xu R, Jackson CM, Tamargo RJ, McDougall CG, et al. Application of unruptured aneurysm scoring systems to a cohort of ruptured aneurysms: are we underestimating rupture risk? *Neurosurg Rev*. 2021;44:3487–98.
9. Neyazi B, Sandalcioğlu IE, Maslehaty H. Evaluation of the risk of rupture of intracranial aneurysms in patients with aneurysmal subarachnoid hemorrhage according to the PHASES score. *Neurosurg Rev*. 2019;42:489–92.
10. Neulen A, Pantel T, König J, Brockmann MA, Ringel F, Kantelhardt SR. Comparison of Unruptured Intracranial Aneurysm Treatment Score and PHASES Score in Subarachnoid Hemorrhage Patients With Multiple Intracranial Aneurysms. *Front Neurol*. 2021;12:616497.
11. Etminan N, Brown RD, Besoglu K Jr, Juvela S, Raymond J, Morita A, et al. The unruptured intracranial aneurysm treatment score: a multidisciplinary consensus. *Neurology*. 2015;85:881–9.
12. Suzuki T, Takao H, Rapaka S, et al. Rupture risk of small unruptured intracranial aneurysms in Japanese adults. *Stroke*. 2020;51:641–3.
13. Murayama Y, Takao H, Ishibashi T, et al. Risk analysis of unruptured intracranial aneurysms: prospective 10-year cohort study. *Stroke*. 2016;47:365–71.
14. Björkman J, Frösen J, Tähtinen O, Backes D, Huttunen T, Harju J, et al. Irregular Shape Identifies Ruptured Intracranial Aneurysm in Subarachnoid Hemorrhage Patients With Multiple Aneurysms. *Stroke*. 2017;48:1986–9.
15. Mehan WA Jr, Romero JM, Hirsch JA, et al. Unruptured intracranial aneurysms conservatively followed with serial CT angiography: could morphology and growth predict rupture? *J Neurointerv Surg*. 2014;6:761–6.
16. Neyazi B, Swiatek VM, Skalej M, Beuing O, Stein KP, Hattungen J, et al. Rupture risk assessment for multiple intracranial aneurysms: why there is no need for dozens of clinical, morphological and hemodynamic parameters. *Ther Adv Neurol Disord*. 2020;13:1756286420966159.
17. Juvela S, Poussa K, Lehto H, Porras M. Natural history of unruptured intracranial aneurysms: a long-term follow-up study. *Stroke*. 2013;44:2414–21.
18. Heit JJ, Gonzalez RG, Sabbag D, Brouwers HB, Ordonez Rubiano EG, Schaefer PW, et al. Detection and characterization of intracranial aneurysms: a 10-year multidetector CT angiography experience in a large center. *J Neurointerv Surg*. 2016;8:1168–72.
19. Kang H, Ji W, Qian Z, Li Y, Jiang C, Wu Z, et al. Aneurysm characteristics associated with the rupture risk of intracranial aneurysms: a self-controlled study. *PLoS ONE*. 2015;10:e0142330.
20. Thompson BG, Brown RD Jr, Amin-Hanjani S, Broderick JP, Cockcroft KM, Connolly ES Jr, et al. Guidelines for the management of patients with unruptured intracranial aneurysms: a guideline for healthcare professionals from the American Heart Association/American Stroke Association. *Stroke*. 2015;46:2368–400.
21. Song JP, Ni W, Gu YX, Zhu W, Chen L, Xu B, et al. Epidemiological Features of Nontraumatic Spontaneous Subarachnoid Hemorrhage in China: A Nationwide Hospital-based Multicenter Study. *Chin Med J (Engl)*. 2017;130:776–81.
22. Wang GX, Wen L, Yang L, Zhang QC, Yin JB, Duan CM, et al. Risk Factors for the Rupture of Intracranial Aneurysms Using Computed Tomography Angiography. *World Neurosurg*. 2018;110:e333–8.
23. Wang GX, Wang S, Liu LL, Gong MF, Zhang D, Yang CY, et al. A Simple Scoring Model for Prediction of Rupture Risk of Anterior Communicating Artery Aneurysms. *Front Neurol*. 2019;10:520.
24. Rajabzadeh-Oghaz H, Wang J, Varble N, Sugiyama SI, Shimizu A, Jing L, et al. Novel Models for Identification of the Ruptured Aneurysm in Patients with Subarachnoid Hemorrhage with Multiple Aneurysms. *AJNR Am J Neuroradiol*. 2019;40:1939–46.
25. Greving JP, Wermer MJ, Brown RD Jr, Morita A, Juvela S, Yonekura M, et al. Development of the PHASES score for prediction of risk of rupture of intracranial aneurysms: a pooled analysis of six prospective cohort studies. *Lancet Neurol*. 2014;13:59–66.
26. Kaminogo M, Yonekura M, Shibata S. Incidence and outcome of multiple intracranial aneurysms in a defined population. *Stroke*. 2002;34:16–21.

Publisher's Note

Springer Nature remains neutral with regard to jurisdictional claims in published maps and institutional affiliations.

Ready to submit your research? Choose BMC and benefit from:

- fast, convenient online submission
- thorough peer review by experienced researchers in your field
- rapid publication on acceptance
- support for research data, including large and complex data types
- gold Open Access which fosters wider collaboration and increased citations
- maximum visibility for your research: over 100M website views per year

At BMC, research is always in progress.

Learn more biomedcentral.com/submissions

